Indonesian Journal of Electrical Engineering and Computer Science
Vol. 34, No. 1, April 2024, pp. 370∼382
ISSN: 2502-4752, DOI: 10.11591/ijeecs.v34.i1.pp370-382

Investigating power scaling factor for pattern division multiple access

Linda Meylani, Vinsensius Sigit Widhi Prabowo, Iswahyudi Hidayat, Nisa Alwiyah
School of Electrical Engineering, Telkom University, Bandung, Indonesia

Article Info

Article history:

Received Nov 13, 2023
Revised Jan 3, 2024
Accepted Jan 14, 2024

Keywords:

Non-othogonal multiple access
Pattern division multiple access
Power scaling factor
Rician fading channels
SIC

ABSTRACT

Pattern division multiple access (PDMA) is a one type of multi-domain non-orthogonal multiple access (NOMA) that support massive connectivity and can improve spectral efficiency. The unique pattern is used by each user to map its transmitting data into a group of resource, which consist of frequency, code and spatial domain or combination of these resources. Power scaling and phase shifting are used to resolve ambiguity as consequence non uniform distribution of the received combined constellation. In this paper, we propose investigation on power scaling factor for each user in PDMA matrix to increase sum rate transmission and propose combine successive interference cancellation (SIC) based on diversity order and power scaling factor for each user. The simulation results confirm that the proper implement power scaling factor in pattern type 2 show best performance in Rician fading channels.

Corresponding Author:
Linda Meylani
School of Electrical Engineering, Telkom University
Bandung, 40275, West Java, Indonesia
Email: lindameylani@telkomuniversity.ac.id

1. INTRODUCTION

The limit of spectrum resources and the growing demand for the internet of things, which makes the future wireless communication technology must be able to support the efficiency of spectrum use and massive connectivity. Non-orthogonal multi access (NOMA) is a new paradigm in multi-access that, with its non-orthogonality, can increase user connectivity. Nowadays, we can divide NOMA into 3 schemes: i) power–domain [1], [2]; ii) code–domain like low density signatures – code division multiple access (LDS–CDMA) [3], low density signature orthogonal frequency division mutiplexing (LDS–OFDM) [4], [5] or sparse code multiple access (SCMA) [6], [7]; and iii) multi–domain such as pattern division multiple access (PDMA) [8]–[11], building block sparse-constellation based orthogonal multiple access (BOMA) [8], [12] and lattice partition multiple access (LPMA) [13]–[15]. Power domain NOMA, we known as PD–NOMA [16], utilizes superposition coding at the transmitter and implements successive interference cancellation (SIC) at the receiver. As one of code–domain NOMA, SCMA apply sparse code book, that is similar to low density signature in LDS–CDMA or LDS–OFDM, to each user/ layer and as a consequence, a certain resource can support more user. Hidayat *et al.* [17], [18] proposed doubly irregular SCMA (DISCMA) that can improve overloading factor more than 300% and also proposed low complexity detection by using peeling decoding. Sharma *et al.* [19] proposed a joint power and code domain NOMA. BOMA [12] connects the information of users with a good channel state information (CSI) to the symbol of a poor CSI user. And, as a results the capacity of a multi-user system has been greatly increased. PDMA is one of multi-domain NOMA [10] based on joint design in transmitter and receiver side. Pattern matrices in PDMA are designed with the variation of diversity order from each user equipment (UE). Therefore, multiple user could ease the error propagation problem of SIC. The pattern designed can be extended by considering the use of power scaling factor and phase shifting. And, in the receiver side, the sparsity nature of the pattern matrix allows the receiver to use advanced detection algorithm such as message passing algorithm (MPA) or SIC that has low complexity as a multi-user detection (MUD).

Research in design of PDMA pattern matrix has been investigated in [10], [20], [21]. Chen *et al.* [10] provide complete explanation about PDMA include principle of PDMA pattern design and extension of PDMA pattern matrix. Ren *et al.* [20] focus to design PDMA pattern matrix for uplink application to massive machine type communication (mMTC) and enhanced mobile broadband (eMBB) and analyse the performance of the proposed pattern matrix using discrete constellation constrained capacity. As further research of [20], [21] focus to design principle and search algorithm both uplink and downlink for mMTC, eMBB, and ultra-reliable and low latency communication (URLLC) in 5G communication system.

Another study on PDMA has done by [22]–[24]. Tang *et al.* [22] studies cooperative PDMA (Co–PDMA) with a half duplex decode and forward (DF) in uplink transmission over Rayleigh fading channel. Research in power allocation has been investigated in [23], [24]. Zeng *et al.* [23] proposed iterative water–filling (IWF) algorithm to allocate power for each user in downlink transmission. While, Zeng *et al.* [24] investigated the optimum power allocation for perfect and non-perfect CSI in downlink transmission.

In this paper, we investigate the impact of power scaling factor in pattern design for uplink PDMA when system use SIC as MUD. The contribution of this paper are summarized as follow:

– Simple power scaling assignment for PDMA pattern design based on R_{gap}.
– Observation on K factor Rician fading channel in term of BER for variation PDMA pattern type and phase shifting.

The rest of this paper is organized as follows. Section 2 describes the system model of PDMA. Section 3 represent implementation of power scaling factor in pattern design. Section 4 provides discussion and analyze the use of power scaling factor in pattern design in PDMA system, and finally, section 5 gives the conclusion of this paper.

2. PDMA: SYSTEM MODELS

In this paper, we consider an uplink transmission of multi-carrier PDMA consist of J user equipments (UE) with user indices $j = 1, 2, 3, ..J$ and N orthogonal resource elements (REs). Without loss of generality, we assume that both transmitter and receiver has a single antenna and we assume that all users take their symbol from the same constellation alphabet $\mathbb{X}$. Each user in PDMA system will transmit its data symbols and spread them into a number of d_{v_i} subcarriers using PDMA pattern. Each of data symbols from each user, therefore, will be multiplied with a unique PDMA pattern g_j. PDMA pattern is represented by element "0" and "1". A $g_{j,n} = 1$ in PDMA pattern represents that data from j-th UE can be mapped into a n-th RE and if $g_{j,n} = 0$ otherwise. System model of PDMA system has shown in Figure 1. In the uplink PDMA, J UE map their transmit data into N orthogonal REs. Block system of uplink transmissin in PDMA has shown in Figure 2.

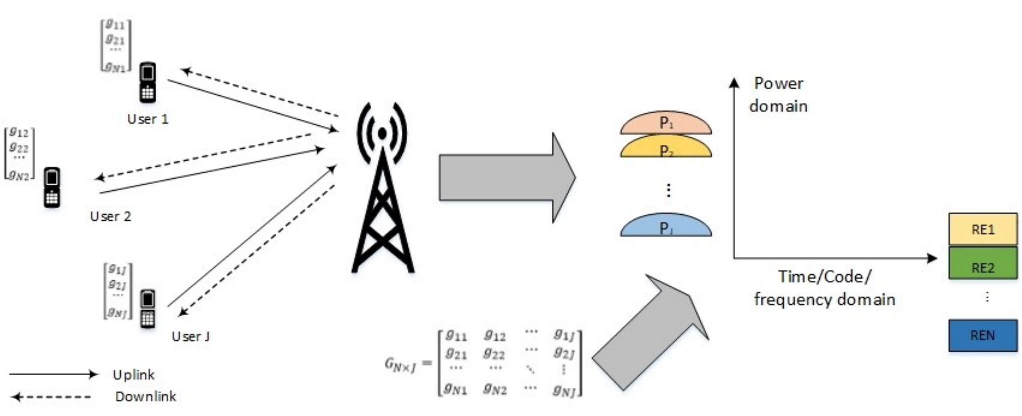

Figure 1. System model of PDMA

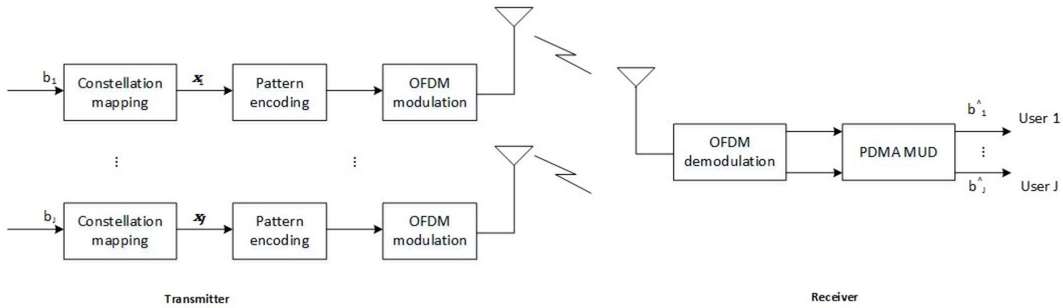

Figure 2. The uplink PDMA

Let the j-th UE transmit data vector x_j that consist of M_j modulated data symbols and stated as:

$$\mathbf{x}_j = (x_{j_1}, x_{j_2}, \cdots, x_{j_{M_j}})^T \tag{1}$$

without loss generality, we assume that all UEs take their symbol from the same constellation alphabet $\mathbf{X}$. In the PDMA system, every UE in the system will transmit its data symbols and spread them into a number of different REs. Therefore, every data symbols from each UE will mutliply with a pattern with low density spreading sequence. Let we assume $\mathbf{g}_j$ as a pattern of the j-th UE, after PDMA encoding process, the j-th UE will have a chips vector, $\mathbf{c}_j$, denotes as:

$$\mathbf{c}_j = x_j \cdot g_j \tag{2}$$

where

$$g_j = w_j \cdot e^{j\beta_j} \tag{3}$$

with w_j and β_j are power scaling factor and phase shifting for each j UE, respectively. In the uplink transmission, each UE will act as trasmitter and in the other side, base station (BS) will act as receiver. The received signal in the n-th RE, y_n at the base station can be represented as:

$$\begin{aligned} y_n &= \sum_{j=1, j \in S_n} \sqrt{p_{j,n}} \cdot \mathbf{c}_{j,n} \cdot h_{j,n} + v_n \\ &= \sum_{j=1, j \in S_n} \sqrt{p_{j,n}} \cdot x_j \cdot g_j \cdot h_{j,n} + v_n \end{aligned} \tag{4}$$

where S_n is a set of UEs accessing the n-th RE and v_n is a AWGN with $\mathcal{N}(0, \sigma_n^2)$.
Assuming CSI is perfect, the throughput of the j-th UE on the n-th RE can be represented as:

$$R_{j,n} = B_{sc} \log_2(1 + \frac{p_{j,n} \cdot x_j \cdot g_j \cdot |h_{j,n}|^2}{\sum_{l=1, l \neq j, l \in S_n} p_{l,n} \cdot x_l \cdot g_l \cdot |h_{l,n}|^2 + \sigma_n^2}) \tag{5}$$

where B_{sc} is a bandwith of each RE.

We assume that PDMA implement PD in the receiver, and PD can perfectly cancell the interference, therefore, the throughput of the last decoded j user can be state as:

$$R_{j,n} = B_{sc} \log_2(1 + \frac{p_{j,n} \cdot x_j \cdot g_j \cdot |h_{j,n}|^2}{\sigma_n^2}) \tag{6}$$

Like on the uplink system, in a downlink transmission, we assume that each user is assigned by a unique PDMA pattern. After PDMA encoding, data streams from all user, x_j, are superimposed and simultaneously transmitted from the BS. The received signal of the j-th UE on the n-th RE can be represented as:

$$y_{j,n} = h_{j,n} g_{j,n} \sqrt{p_{j,n}} x_{j,n} + h_{j,n} \sum_{l=1, l \neq j}^{J} g_{l,n} \sqrt{p_{j,n}} x_{l,n} + v_{j,n} \quad (7)$$

where $h_{j,n}$ is a downlink channel gain of j-th user at the n-th RE, $g_{j,n}$ is a pattern of j-th user at the n-th RE, $x_{j,n}$ is a modulated symbol of j-th user at the n-th RE and $v_{j,n}$ is a Gaussian random noise of the j-th user at the n-th RE with zero mean and variance σ_n^2. The downlink block system has shown in Figure 3.

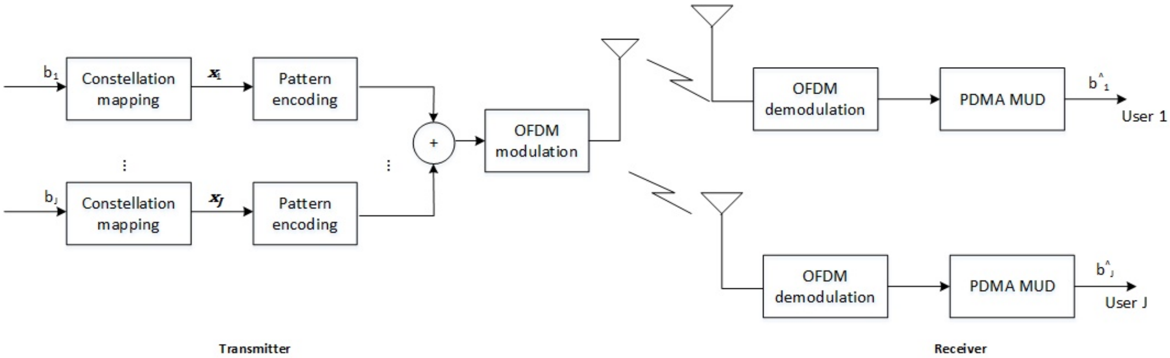

Figure 3. Downlink PDMA

By taking interference from other user that access the same resource into account, the throughput of the j-th on the n RE in downlink transmission can be defined as:

$$R_{j,n} = B_{sc} \log_2 (1 + \frac{p_{j,n} \cdot x_j \cdot g_j \cdot |h_{j,n}|^2}{\sum_{l=1, l \neq j, l \in S_n} p_{l,n} \cdot x_l \cdot g_l \cdot h_{j,n}|^2 + \sigma_n^2}) \quad (8)$$

However when PDMA system implement PD to decode symbols of all users, and by assume that PD can cancel the interference perfectly, then the throughput of the last decoded user (with the lowest power factor) can be represented as:

$$R_{j,n} = B_{sc} \log_2 (1 + \frac{p_{j,n} \cdot x_j \cdot g_j \cdot |h_{j,n}|^2}{\sigma_n^2}) \quad (9)$$

3. PDMA PATTERN DESIGN

Each UE in PDMA has a unique pattern and each group in PDMA consists of a number of UEs with the same diversity order. In this paper, we use R_{gap}, a gap ratio of the power of detected UE to the interference, to determine the power scaling factor for each group and each UE on the design of UE's pattern. In this section, power scaling factor is proposed to maximize the sum throughput of PDMA system in uplink and downlink transmission and to support decoding process using SIC. Tse and Hanly [25], showed that the optimization of power allocation for multi user can be applied in each frequency. In this paper, investigate 4 type of power scaling factor. In the first type, different group will have different value of power scaling, and we allocate the same power scaling for each user in the same group. Each user has the same power scaling factor in each RE.

Assume that there are 6 UEs and 4 REs in PDMA system with a pattern G [21], has been shown in (10),

$$G = \begin{bmatrix} 1 & 0 & 1 & 1 & 1 & 0 \\ 0 & 0 & 1 & 1 & 1 & 1 \\ 0 & 0 & 1 & 1 & 1 & 1 \\ 0 & 1 & 1 & 1 & 0 & 1 \end{bmatrix} \quad (10)$$

Matrix G has 3 groups of UE with different diversity orders, the 3rd and 4th users are in the same group with diversity order 4, the 5th and 6th UEs are in the same group, and the last group with diversity order 1 consist of 2 user, 1st and 2nd user. Higher power scaling factor will be allocated to UEs with higher diversity orders. In the uplink transmission, the received signal in the first REs at BS can be represented in (11).

$$\begin{aligned} y_1 &= \sqrt{p}\sqrt{\rho_{g_3}}\exp^{j\beta_1}\ x_{1,1}h_{1,1} + \sqrt{p}\sqrt{\rho_{g_{1,1}}}\exp^{j\beta_3} x_{3,1}h_{3,1} \\ &+ \sqrt{p}\sqrt{\rho_{g_{1,4}}}\exp^{j\beta_4} x_{4,1}h_{4,1} + \sqrt{p}\sqrt{\rho_{g_{2,1}}}\exp^{j\beta_5} x_{5,1}h_{5,1} + v_1 \end{aligned} \quad (11)$$

where $\rho_{g_{do}}$ is a power scaling factor for a grup of do diversity order and $\rho_{g_1} > \rho_{g_2} > \rho_{g_3}$.

To perform interference cancellation using SIC in the receiver, power scaling factor for all UE must manage properly. Ali *et al.* [26] state P_{gap} as a minimum power difference required to perform interference cancellation properly, which is obtained from the difference between power of the signal to be decoded and the remaining non–decoded signals. Due to our system works in multi–carrier system, we defined R_{gap} instead of P_{gap} to adjust the power scaling factor of each UE on each RE and to ensure SIC can work properly. The R_{gap} is used to control the power scaling factor for each group of diversity order. And, the R_{gap} in the first RE can define as:

$$R_{gap} = \frac{\rho_{g_1}}{\rho_{g_1} + \rho_{g_2} + \rho_{g_3}} \quad (12)$$

and

$$R_{gap} = \frac{\rho_{g_2}}{\rho_{g_2} + \rho_{g_3}} \quad (13)$$

In this paper, we propose 4 types of PDMA pattern base on allocating power scaling dan phase shifting. The rules of allocating power scaling for each user is different for each type, as shown in Tables 1 and 2. Type 1 and type 2 assign power scaling for each UE based on group of diversity order. Group with high diversity order will assign with higher power scaling factor. In the type 1, each UE in the same group of diversity order has the same power scaling factor, where the value of the power scaling factor of each UE is the power scaling of the diversity group divided by the number of active UE in RE. As shown in the Table 3, UE 3 and UE 4 in type 1 has the same power scaling, $\frac{\rho_{g1}}{2}$. And UE 5 and UE 6 in the 2nd RE will have the same power scaling, $\frac{\rho_{g2}}{2}$. Different with type 1, in the type 2, we propose scaling factor for each user in the same group. If power scaling group are state as ρ_{g_1}, ρ_{g_2} and ρ_{g_3}, where $\rho_{g_1} > \rho_{g_2} > \rho_{g_3}$, therefore, by using scaling factor in each group, UE 3 and UE 4 will have power scaling factor as state as $\alpha_3 = \rho_{g_{1,1}}$ and $\alpha_4 = \rho_{g_{1,2}}$.

Table 1. The rules of allocating power scaling for type 1 and type 2

	The rules of allocating power scaling for type 1		The rules of allocating power scaling for type 2
1	Group UE based on diversity order. Count number of group, G.	1	Group UE based on diversity order. Count number of group, G.
2	Determine R_{gap}	2	Determine R_{gap}
3	Count the power scaling factor for each group $$\rho_{g_{do}} = R_{gap} \cdot (1 - R_{gap})^{do-1}$$ $do = 1, 2, \cdots, G-1$ power scaling factor for group with lowest diversity order $$\rho_{g_G} = \frac{\rho_{g_{G-1}}}{R_{gap}} \cdot (1 - R_{gap})$$	3	Count the power scaling factor for each group $$\rho_{g_{do}} = R_{gap} \cdot (1 - R_{gap})^{do-1}$$ $do = 1, 2, \cdots, G-1$ power scaling factor for group with lowest diversity order $$\rho_{g_G} = \frac{\rho_{g_{G-1}}}{R_{gap}} \cdot (1 - R_{gap})$$
4	if Group has K UEs, than, power scaling for each UE in one group is represented as $$\alpha_k = \frac{\rho_{g_{do}}}{K}$$ If member of group *do* only one UE $$\alpha_k = \rho_{g_{do}}$$	4	if group has K UEs, than, power scaling for each UE in one group is represented as $$\alpha_k = \rho_{g_G} \cdot R_{gap} \cdot (1 - R_{gap})^{k-1}$$ power scaling factor for last UE in a group $$\alpha_K = \rho_{g_G} \cdot \frac{\alpha_{K-1}}{R_{gap}} \cdot (1 - R_{gap})$$

Table 2. The rules of allocating power scaling for type 3 and type 4

	The rules of allocating power scaling for type 3		The rules of allocating power scaling for type 4
1	Group UE based on diversity order. Count number of group, G.	1	Count number of UEs in a RE, K
2	Determine R_{gap}	2	Determine R_{gap}
3	Count the power scaling factor for each group $$\rho_{g_{do}} = R_{gap} \cdot (1 - R_{gap})^{do-1}$$ $do = 1, 2, \cdots, G-1.$ power scaling factor for group with lowest diversity order $$\rho_{g_G} = \frac{\rho_{g_{G-1}}}{R_{gap}} \cdot (1 - R_{gap})$$	3	Count the power scaling factor for each UE $$\alpha_k = R_{gap} \cdot (1 - R_{gap})^{k-1}$$ $k = 1, 2, \cdots, K-1$ power scaling factor for last UE in RE $$\alpha_K = \frac{\alpha_{K-1}}{R_{gap}} \cdot (1 - R_{gap})$$
4	if Group has K UEs, than, power scaling for each UE in one Group is represented as $$\alpha_k = \frac{\rho_{g_{do}}}{K}$$	4	Assign each UE in first RE with specific power scaling based on step 3.
5	for first RE, assign each UE with spesific power scaling based on step 3 and step 4.		Re-assign different power scaling for each UE in other RE by fulfill (14).
6	For 2nd, and other RE, re-assign different power scaling for each UE by fulfill (14).		

Table 3. Power scaling in PDMA pattern type

Power scaling type	PDMA Pattern	
Type 1	$\begin{bmatrix} \sqrt{\rho_{g_3}} & 0 & \sqrt{\rho_{g_1}/2} & \sqrt{\rho_{g_1}/2} & \sqrt{\rho_{g_2}} & 0 \\ 0 & 0 & \sqrt{\rho_{g_1}/2} & \sqrt{\rho_{g_1}/2} & \sqrt{\rho_{g_2}/2} & \sqrt{\rho_{g_2}/2} \\ 0 & 0 & \sqrt{\rho_{g_1}/2} & \sqrt{\rho_{g_1}/2} & \sqrt{\rho_{g_2}/2} & \sqrt{\rho_{g_2}/2} \\ 0 & \sqrt{\rho_{g_3}} & \sqrt{\rho_{g_1}/2} & \sqrt{\rho_{g_1}/2} & 0 & \sqrt{\rho_{g_2}} \end{bmatrix}$	$\sqrt{\rho_{g_1}} > \sqrt{\rho_{g_2}} > \sqrt{\rho_{g_3}}$
Type 2	$\begin{bmatrix} \sqrt{\rho_{g_3}} & 0 & \sqrt{\rho_{g_{1,1}}} & \sqrt{\rho_{g_{1,2}}} & \sqrt{\rho_{g_2}} & 0 \\ 0 & 0 & \sqrt{\rho_{g_{1,1}}} & \sqrt{\rho_{g_{1,2}}} & \sqrt{\rho_{g_{2,1}}} & \sqrt{\rho_{g_{2,1}}} \\ 0 & 0 & \sqrt{\rho_{g_{1,1}}} & \sqrt{\rho_{g_{1,2}}} & \sqrt{\rho_{g_{2,1}}} & \sqrt{\rho_{g_{2,1}}} \\ 0 & \sqrt{\rho_{g_3}} & \sqrt{\rho_{g_{1,1}}} & \sqrt{\rho_{g_{1,2}}} & 0 & \sqrt{\rho_{g_2}} \end{bmatrix}$	$\sqrt{\rho_{g_{1,1}}} > \sqrt{\rho_{g_{1,2}}}$
Type 3	$\begin{bmatrix} \sqrt{\rho_{g_3}} & 0 & \sqrt{\rho_{g_1}/2} & \sqrt{\rho_{g_1}/2} & \sqrt{\rho_{g_2}} & 0 \\ 0 & 0 & \sqrt{\rho_{g_2}/2} & \sqrt{\rho_{g_2}/2} & \sqrt{\rho_{g_1}/2} & \sqrt{\rho_{g_1}/2} \\ 0 & 0 & \sqrt{\rho_{g_3}/2} & \sqrt{\rho_{g_3}/2} & \sqrt{\rho_{g_2}/2} & \sqrt{\rho_{g_2}/2} \\ 0 & \sqrt{\rho_{g_2}} & \sqrt{\rho_{g_3}/2} & \sqrt{\rho_{g_3}/2} & 0 & \sqrt{\rho_{g_3}} \end{bmatrix}$	
Type 4	$\begin{bmatrix} \sqrt{\alpha_{1,1}} & 0 & \sqrt{\alpha_{3,1}} & \sqrt{\alpha_{4,1}} & \sqrt{\alpha_{5,1}} & 0 \\ 0 & 0 & \sqrt{\alpha_{3,2}} & \sqrt{\alpha_{4,2}} & \sqrt{\alpha_{5,2}} & \sqrt{\alpha_{6,2}} \\ 0 & 0 & \sqrt{\alpha_{3,3}} & \sqrt{\alpha_{4,3}} & \sqrt{\alpha_{5,3}} & \sqrt{\alpha_{6,3}} \\ 0 & \sqrt{\alpha_{2,4}} & \sqrt{\alpha_{3,4}} & \sqrt{\alpha_{4,4}} & 0 & \sqrt{\alpha_{6,4}} \end{bmatrix}$	

In type 3, similar to type 1, different power scaling for each group of diversity orders is still used. However, in different REs, each group will have a different power scaling factor. And, in the type 4, we propose power scaling based on the number of active UE in each RE, not based on a group of diversity order. The power scaling factor for each UE in each RE will be different. The important requirements that must be met in each RE are:

$$\sum_{j \in S_n} \alpha_{j,n} = 1 \tag{14}$$

Let $\alpha_{j,n}$ as a power scaling of UE j at RE n, therefore, the PDMA pattern for (10) can be define as:

$$G = \begin{bmatrix} \sqrt{\alpha_{1,1}} & 0 & \sqrt{\alpha_{3,1}} & \sqrt{\alpha_{4,1}} & \sqrt{\alpha_{5,1}} & 0 \\ 0 & 0 & \sqrt{\alpha_{3,2}} & \sqrt{\alpha_{4,2}} & \sqrt{\alpha_{5,2}} & \sqrt{\alpha_{6,2}} \\ 0 & 0 & \sqrt{\alpha_{3,3}} & \sqrt{\alpha_{4,3}} & \sqrt{\alpha_{5,3}} & \sqrt{\alpha_{6,3}} \\ 0 & \sqrt{\alpha_{2,4}} & \sqrt{\alpha_{3,4}} & \sqrt{\alpha_{4,4}} & 0 & \sqrt{\alpha_{6,4}} \end{bmatrix} \quad (15)$$

In this paper, we assume each user uses different phase shift, therefore PDMA pattern in (15) be state as:

$$G = \begin{bmatrix} \sqrt{\alpha_{1,1}} \cdot \exp^{j\beta_1} & 0 & \sqrt{\alpha_{3,1}} \cdot \exp^{j\beta_3} & \sqrt{\alpha_{4,1}} \cdot \exp^{j\beta_4} & \sqrt{\alpha_{5,1}} \cdot \exp^{j\beta_5} & 0 \\ 0 & 0 & \sqrt{\alpha_{3,2}} \cdot \exp^{j\beta_3} & \sqrt{\alpha_{4,2}} \cdot \exp^{j\beta_4} & \sqrt{\alpha_{5,2}} \cdot \exp^{j\beta_5} & \sqrt{\alpha_{6,2}} \cdot \exp^{j\beta_6} \\ 0 & 0 & \sqrt{\alpha_{3,3}} \cdot \exp^{j\beta_3} & \sqrt{\alpha_{4,3}} \cdot \exp^{j\beta_4} & \sqrt{\alpha_{5,3}} \cdot \exp^{j\beta_5} & \sqrt{\alpha_{6,3}} \cdot \exp^{j\beta_6} \\ 0 & \sqrt{\alpha_{2,4}} \cdot \exp^{j\beta_2} & \sqrt{\alpha_{3,4}} \cdot \exp^{j\beta_3} & \sqrt{\alpha_{4,4}} \cdot \exp^{j\beta_4} & 0 & \sqrt{\alpha_{6,4}} \cdot \exp^{j\beta_6} \end{bmatrix} \quad (16)$$

4. RESULTS AND DISCUSSION

In this section, we evaluate the impact of power scaling factors on PDMA patterns. At the receiver, SIC is used to decode all receiver symbols for all users. The process starts from the EU with a high diversity order. To evaluate the performance of the power scaling pattern, this paper uses the pattern matrix 3×7 in [11] by changing the non-zero elements to ones as shown in (17).

$$S = \begin{bmatrix} 1 & 1 & 0 & 1 & 1 & 0 & 0 \\ 1 & 1 & 1 & 0 & 0 & 1 & 0 \\ 1 & 0 & 1 & 1 & 0 & 0 & 1 \end{bmatrix} \quad (17)$$

In pattern matrix, S, there are three groups with different diversity orders. UE 1 has the highest diversity order of 3, UE 2–4 have diversity order of 2 and UE 5–7 have diversity order of 1. In this section, we evaluate 4 types of power scaling factors in Table 3 in Rician fading channels. In this paper, phase shifting is used to minimize ambiguity when decoding the receiving symbols. The transmitted symbols of each UE in the same group will be differentiated based on different phase shift. Figure 4 shows the impact of power scaling factor and phase shifting to the formed constellation of 3 UEs when transmit symbols. This figure shows that power scaling and phase shift will affect the density between symbols and the number of constellation points that may be formed. Figure 4(a) shows the formed constellation points when all three users use the same power scaling factor (all users use $\sqrt{\alpha} = 1$) and use BPSK as a modulation type. From this figure, there are 4 formed constellation points as a combination of 3 users with the same power. In the other sides, Figures 4(b) to 4(d) show the formed of constellation points when 3 users use different value of phase shifting or power scaling. This figures show that there are more formed constellation points rather than Figure 4(a). Moreover, variations in power scaling will result in smaller minimum distances between symbols.

In this paper, we evaluate the leverage of power scaling in PDMA pattern when simulated in Rician fading channels. The simulation parameter are shown in Table 4. Due to the maximum number of UEs in each RE are four UEs, therefore there are 4 phase shifts will be implemented. And, each UE will uses a different phase shift. In our system, we assume transmiter and receiver have knowledge of each other, especially the power scaling that used by each user. SIC is used to decode received symbols of all users and the decoding process start from user with higher diversity order. However, system will not decode symbols in all resources. In this systems, receiver will decode symbols from resource with higher power scaling factor. Figure 5 show the performance of PDMA with variation pattern types in uplink and downlink transmission at Rician Fading channel with $K = 5$ dB.

Rician fading channel is one of the stochastic models for radio propagation. The Rician channel is remarkably similar to the Rayleigh fading channel except for the presence of a dominant component from line-of-sight (LOS) waves. K factor in Rician channels represent the ratio of power of the LOS component to the power of the scattered components. The worst case Rician channels associated with $K = 0$. In this condition, Rician channels represent Rayleigh channel with no LOS path. While Rician channels has $K = \infty$, it represent Gaussian channels with strong LOS component. In this paper, we evaluate the performance of PDMA pattern in two value of K factor, i.e., $K = 5$ dB and $K = 20$ dB. When $K = 5$ dB, as shown in Figure 5(a), PDMA has poor performance in uplink transmission compare to downlink transmission as shown in Figure 5(b). Nevertheless, in general, pattern type 2 has better performance compare to others types due to the used of double power scaling, i.e. power scaling in a group of diversity order and power scaling for UEs in the same group. In Figure 5(b), pattern type 2 and type 3 show similar performance. Although pattern type 3 do not use double scaling, however, in this pattern each user is assigned different power scaling in different RE. Therefore, increasing the possibility of other users to obtain higher value of power scaling to improve detection performance. To obtain BER 10^{-4}, PDMA pattern type 2 needs average SNR until 24 dB in uplink transmission while in downlink transmission its only need 22.5 dB. Performance of PDMA at Rician fading when $K = 20$ dB has shown in Figure 6. Performance of PDMA in uplink and downlink transmission at Rician fading with $K = 20$ dB have shown in Figure 6(a) and Figure 6(b), respectively. Performance stability has shown by PDMA pattern type 2, where it has better performance compare to other types. In this case, by using doubly power scaling to assign power to each user, PDMA can have better performance.

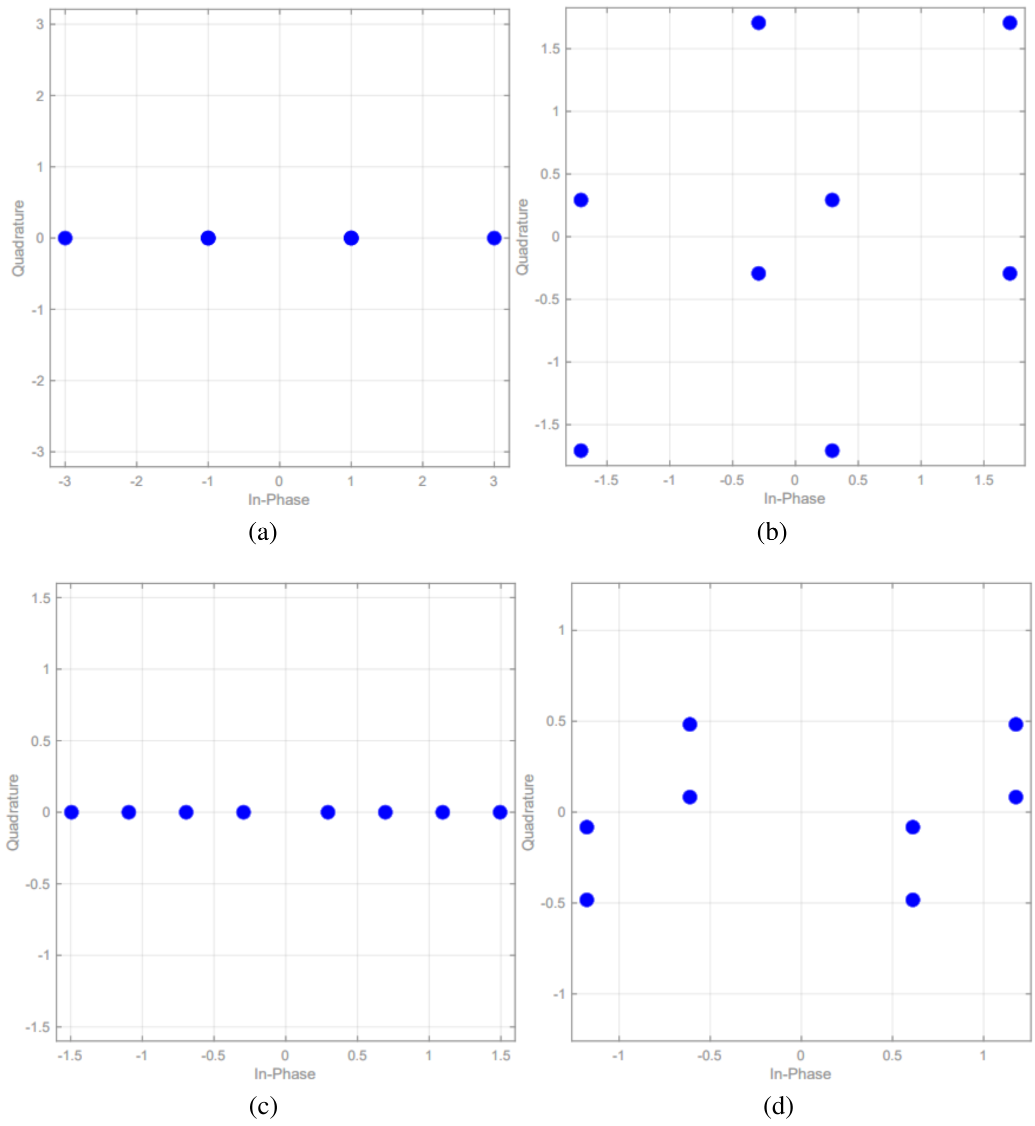

Figure 4. The formed constellation from combination of 3 users: (a) with the same power scaling factor $\{1\}$ and the phase shift $\{0\}$, (b) same power scaling $\{1\}$ with different phase shift$\{0, \frac{pi}{4}, \frac{2\pi}{4}\}$, (c) with the same phase shift $\{0\}$ and different power scaling factor $\{0.8, 0.16, 0.04\}$, and (d) dan different power scaling $\{0.8, 0.16, 0.04\}$ and different phase shift $\{0, \frac{pi}{4}, \frac{2\pi}{4}\}$

Table 4. Simulation parameter

Parameter	PDMA
Pattern matrix	S
Power scaling factor in each RE	$\sum_{j\in S_n}\alpha_{j,n}=1$
Phase shifter	$\frac{\pi}{4}\{0,\frac{\pi}{4},\frac{2\pi}{4},\frac{3\pi}{4}\}$
	$\frac{\pi}{5}\{0,\frac{\pi}{5},\frac{2\pi}{5},\frac{3\pi}{5}\}$
	$\frac{\pi}{6}\{0,\frac{\pi}{6},\frac{2\pi}{6},\frac{3\pi}{6}\}$
	$0\{0,0,0\}$
R_{gap}	0.8; 0.85; 0.9
Number of UE	7
Number of resources	3
Fading channels	Rician fading channels with $K=5$ dB and $K=20$ dB

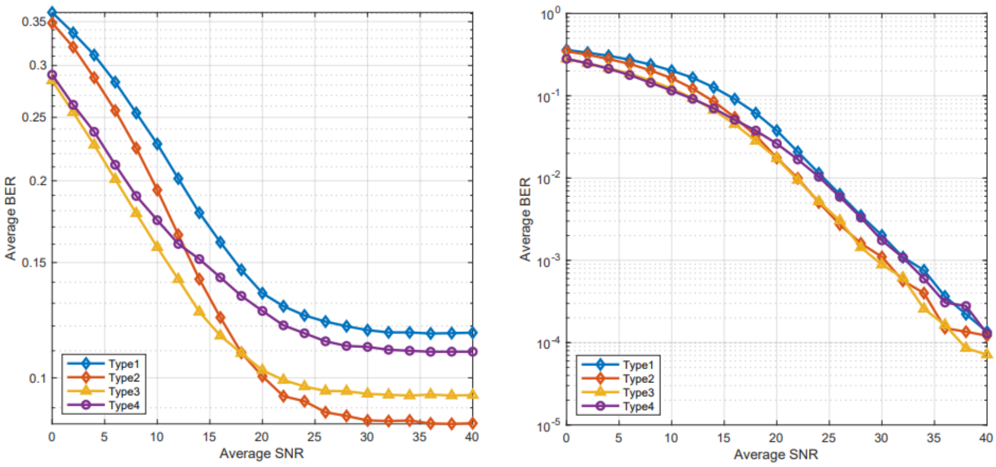

(a) (b)

Figure 5. Comparison performance of PDMA pattern with phase 1 in (a) uplink and (b) downlink Rician fading channel with $K=5$ dB

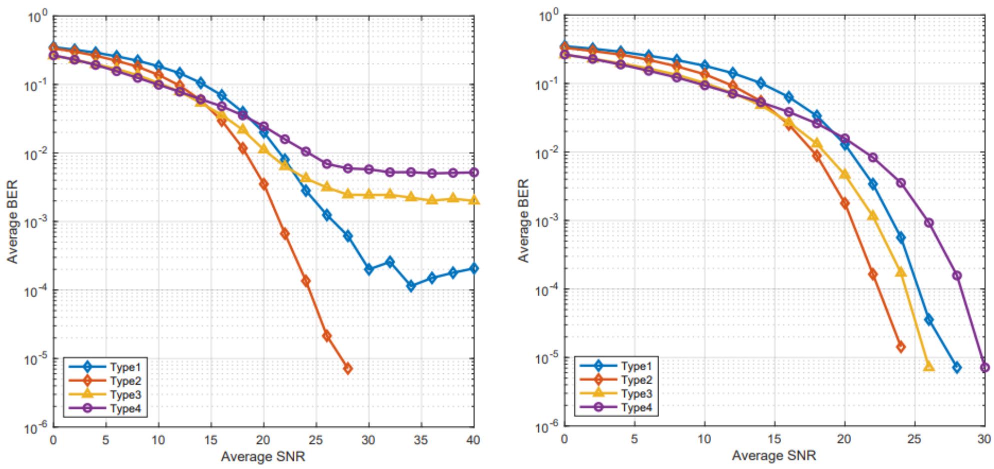

(a) (b)

Figure 6. Comparison performance of PDMA pattern with phase 1 in (a) uplink and (b) downlink Rician fading channel with $K=20$ dB

Figure 7 shows the impact of variation value of R_{gap} to the performance of PDMA pattern at Rician fading channels. In this section, we compare 3 values of $R_{gap}=\{0.8;0.85,0.9\}$ to the performance of PDMA.

Figures 7(a) and 7(b) show the performance of PDMA pattern type 2 in uplink and downlink transmission at Rician fading channel with $K = 20dB$, respectively. These figures show that R_{gap} can predispose the performance of the PDMA system. In our cases, a higher value of R_{gap} makes the average PDMA system performance become worse. In our scheme, when R_{gap} is set to be a higher value, UE with higher diversity order will obtain a higher power weighted factor, and have a good performance cause other UE that access the same RE is treated as a noise with a lower power scaling factor. Unfortunately, UE with the lowest diversity order (this UE has the lowest power scaling factor) has the worst performance. Performance of all user has shown in Figure 8. As shown in Figure 8(a), at $R_{gap} = 0.8$, for average BER target 10^{-4}, UE 1 only need SNR 13.5 dB, however, UE 7 need higher SNR 23 dB to achieve same BER. On the other side, as shown in Figure 8(b), when $R_{gap} = 0.9$ is used to set the power scaling factor, UE 1 needs more lower SNR to achieve BER 10^{-4} rather than in $R_{gap} = 0.8$. And, UE 7 needs more higher SNR (30 dB) to obtain the BER target.

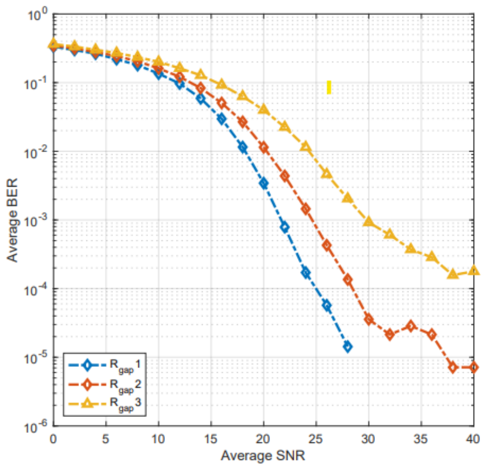

(a) (b)

Figure 7. Comparison performance of PDMA pattern type 2 in (a) uplink and (b) downlink transmission at Rician fading channel with $K = 20$

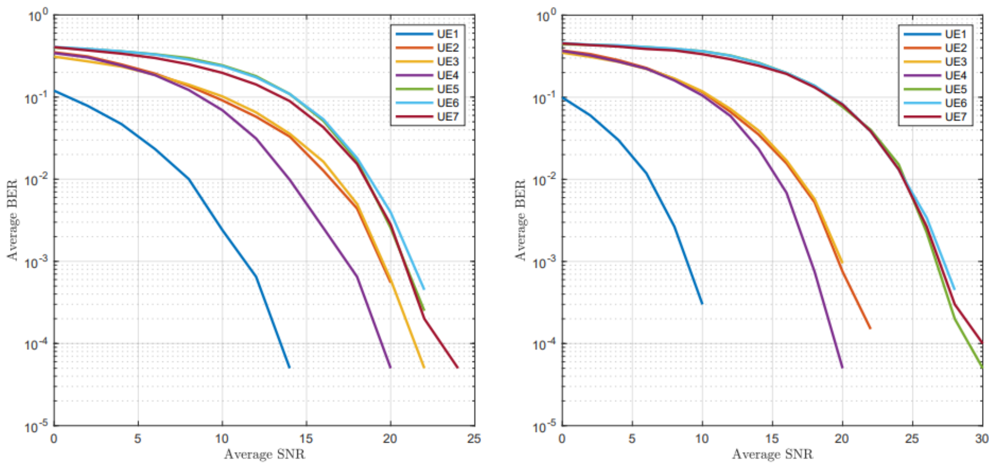

(a) (b)

Figure 8. Performance of all UE in downlink transmission at Rician fading channel with $K = 20$ with (a) $R_{gap} = 0.8$ dan (b) $R_{gap} = 0.9$

In this section, we also investigate the impact of phase shifting to PDMA's performance as shown in Figure 9. Figures 9(a) and 9(b) show the impact of phase shifting to the performance of PDMA pattern type 2.

It seem phase shift 1, $\frac{\pi}{4}$, has a better performance than phase 2, $\frac{\pi}{5}$, or phase 3, $\frac{\pi}{6}$, and phase 4. The use of phase shift is intended to avoid ambiguity in the decoding process. It can be seen that when all UEs accessing the same RE use the same phase shifting (or all UE implement no phase shifting), PDMA performance of phase 4 becomes worse. In this section, we also compare performance of the proposed pattern type 2 with PDMA's patterns for eMBB and URLLC in [21], and receiver decode all transmitting symbol of all UEs by using SIC. Decoding process start with UE with higher diversity order. The simulation results ,as shown in Figure 10, confirm that the proposed pattern based on scaling factor has better performance compare to the eMBB and URLLC patterns in [21], due to decoding process start form UE with high diversity order. And in the proposed pattern, UE with higher diversity order has higher power scaling factor.

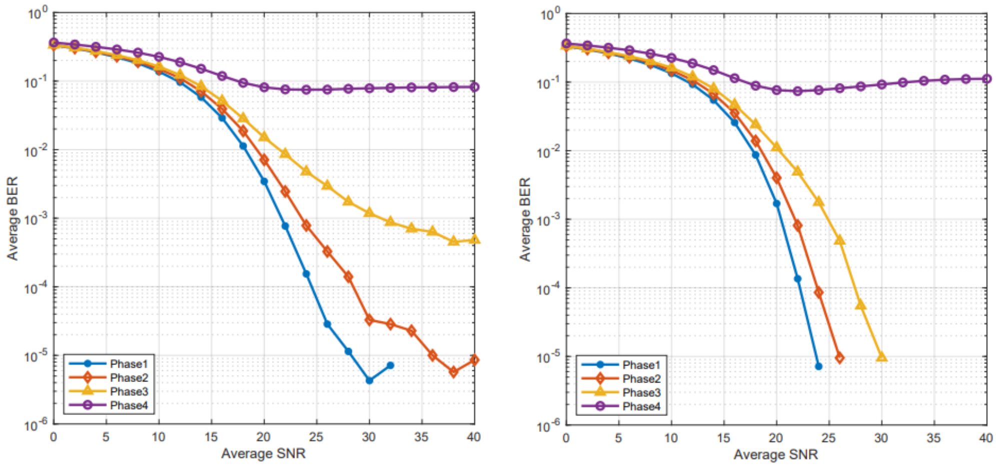

(a) (b)

Figure 9. The impact of phase shifting in PDMA for pattern type 2 in (a) uplink and (b) downlink transmission at Rician fading channel with $K = 20$

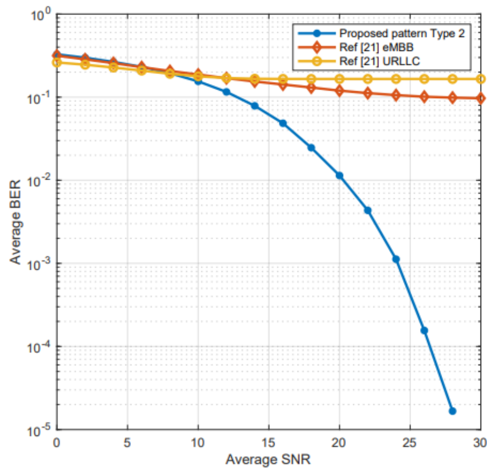

Figure 10. Performance of the proposed PDMA type 2 compare with PDMA pattern for eMBB and URLLC in [21]

5. CONCLUSION

In this paper, we investigate the effect of the power scaling factor and phase shifting on a pattern of UE to the PDMA system. Our simulation confirmed both phase shifting and power scaling factors can influence the PDMA performance. Based on the observation, pattern type 2 has better performance than other types. This pattern used scaling power factor not only on a group of diversity order but also on each user in the same group. A higher value of R_{gap} has an impact on increasing the performance gap for each group diversity order. A higher value of R_{gap} has an impact on a larger performance gap in each group diversity order, and results in a decrease in the average performance of the PDMA system.

ACKNOWLEDGEMENTS

This research was financially supported by The Ministry of Education, Culture, Research and Technology, Indonesia with Grant No. 003/SP2H/RT-MONO/LL4/2023 and 339/PNLT2/PPM/2023.

REFERENCES

[1] Y. Saito, Y. Kishiyama, A. Benjebbour, T. Nakamura, A. Li, and K. Higuchi, "Non-orthogonal multiple access (NOMA) for cellular future radio access," in *2013 IEEE 77th Vehicular Technology Conference (VTC Spring)*, Jun. 2013, pp. 1–5, doi: 10.1109/VTC-Spring.2013.6692652.

[2] A. Benjebbour, Y. Saito, Y. Kishiyama, A. Li, A. Harada, and T. Nakamura, "Concept and practical considerations of non-orthogonal multiple access (NOMA) for future radio access," in *2013 International Symposium on Intelligent Signal Processing and Communication Systems*, Nov. 2013, pp. 770–774, doi: 10.1109/ISPACS.2013.6704653.

[3] R. Hoshyar, F. P. Wathan, and R. Tafazolli, "Novel low-density signature for synchronous CDMA systems over AWGN channel," *IEEE Transactions on Signal Processing*, vol. 56, no. 4, pp. 1616–1626, Apr. 2008, doi: 10.1109/TSP.2007.909320.

[4] R. Hoshyar, R. Razavi, and M. Al-Imari, "LDS-OFDM an efficient multiple access technique," in *2010 IEEE 71st Vehicular Technology Conference*, 2010, pp. 1–5, doi: 10.1109/VETECS.2010.5493941.

[5] R. Razavi, M. AL-Imari, M. A. Imran, R. Hoshyar, and D. Chen, "On receiver design for uplink low density signature OFDM (LDS-OFDM)," *IEEE Transactions on Communications*, vol. 60, no. 11, pp. 3499–3508, Nov. 2012, doi: 10.1109/TCOMM.2012.082812.110284.

[6] H. Nikopour and H. Baligh, "Sparse code multiple access," in *2013 IEEE 24th Annual International Symposium on Personal, Indoor, and Mobile Radio Communications (PIMRC)*, Sep. 2013, pp. 332–336, doi: 10.1109/PIMRC.2013.6666156.

[7] M. Taherzadeh, H. Nikopour, A. Bayesteh, and H. Baligh, "SCMA codebook design," in *2014 IEEE 80th Vehicular Technology Conference (VTC2014-Fall)*, Sep. 2014, pp. 1–5, doi: 10.1109/VTCFall.2014.6966170.

[8] Y. Cai, Z. Qin, F. Cui, G. Y. Li, and J. A. McCann, "Modulation and multiple access for 5G networks," *IEEE Communications Surveys & Tutorials*, vol. 20, no. 1, pp. 629–646, 2018, doi: 10.1109/COMST.2017.2766698.

[9] J. Zeng, B. Li, X. Su, L. Rong, and R. Xing, "Pattern division multiple access (PDMA) for cellular future radio access," in *2015 International Conference on Wireless Communications & Signal Processing (WCSP)*, Oct. 2015, pp. 1–5, doi: 10.1109/WCSP.2015.7341229.

[10] S. Chen, B. Ren, Q. Gao, S. Kang, S. Sun, and K. Niu, "Pattern division multiple access—a novel nonorthogonal multiple access for fifth-generation radio networks," *IEEE Transactions on Vehicular Technology*, vol. 66, no. 4, pp. 3185–3196, Apr. 2017, doi: 10.1109/TVT.2016.2596438.

[11] X. Dai, Z. Zhang, B. Bai, S. Chen, and S. Sun, "Pattern division multiple access: a new multiple access technology for 5G," *IEEE Wireless Communications*, vol. 25, no. 2, pp. 54–60, Apr. 2018, doi: 10.1109/MWC.2018.1700084.

[12] M. A. Naim, J. P. Fonseka, and E. M. Dowling, "A building block approach for designing multilevel coding schemes," *IEEE Communications Letters*, vol. 19, no. 1, pp. 2–5, Jan. 2015, doi: 10.1109/LCOMM.2014.2364190.

[13] D. Fang, Y.-C. Huang, Z. Ding, G. Geraci, S.-L. Shieh, and H. Claussen, "Lattice partition multiple access: a new method of downlink non-orthogonal multiuser transmissions," in *2016 IEEE Global Communications Conference (GLOBECOM)*, Dec. 2016, pp. 1–6, doi: 10.1109/GLOCOM.2016.7841947.

[14] M. Qiu, Y.-C. Huang, S.-L. Shieh, and J. Yuan, "A lattice-partition framework of downlink non-orthogonal multiple access without SIC," *IEEE Transactions on Communications*, vol. 66, no. 6, pp. 2532–2546, Jun. 2018, doi: 10.1109/TCOMM.2018.2805895.

[15] M. Qiu, Y.-C. Huang, J. Yuan, and C.-L. Wang, "Lattice-partition-based downlink non-orthogonal multiple access without SIC for slow fading channels," *IEEE Transactions on Communications*, vol. 67, no. 2, pp. 1166–1181, Feb. 2019, doi: 10.1109/TCOMM.2018.2878847.

[16] S. M. R. Islam, N. Avazov, O. A. Dobre, and K. Kwak, "Power-domain non-orthogonal multiple access (NOMA) in 5G systems: potentials and challenges," *IEEE Communications Surveys & Tutorials*, vol. 19, no. 2, pp. 721–742, 2017, doi: 10.1109/COMST.2016.2621116.

[17] I. Hidayat, L. Meylani, A. Kurniawan, M. S. Arifianto, and K. Anwar, "Doubly irregular sparse code multiple access with EXIT analysis," in *2018 International Conference on Signals and Systems (ICSigSys)*, May 2018, pp. 115–119, doi: 10.1109/ICSIGSYS.2018.8372648.

[18] I. Hidayat, L. Meylani, A. Kurniawan, M. S. Arifianto, and K. Anwar, "Practical decoding scheme for doubly irregular sparse code multiple access," in *2019 26th International Conference on Telecommunications (ICT)*, Apr. 2019, pp. 135–141, doi: 10.1109/ICT.2019.8798822.

[19] S. Sharma, K. Deka, V. Bhatia, and A. Gupta, "Joint power-domain and SCMA-based NOMA system for downlink in 5G and beyond," *IEEE Communications Letters*, vol. 23, no. 6, pp. 971–974, Jun. 2019, doi: 10.1109/LCOMM.2019.2911082.

[20] B. Ren, Y. Wang, X. Dai, K. Niu, and W. Tang, "Pattern matrix design of PDMA for 5G UL applications," *China Communications*, vol. 13, no. 2, pp. 159–173, 2016, doi: 10.1109/CC.2016.7405732.

[21] J. Sun, C. Wang, J. Zeng, X. Su, and T. Lv, "Design of PDMA pattern matrix in 5G scenarios," in *2020 IEEE 91st Vehicular Technology Conference (VTC2020-Spring)*, May 2020, pp. 1–6, doi: 10.1109/VTC2020-Spring48590.2020.9129446.

[22] W. Tang, S. Kang, and B. Ren, "Performance analysis of cooperative pattern division multiple access (Co-PDMA) in uplink network," *IEEE Access*, vol. 5, pp. 3860–3868, 2017, doi: 10.1109/ACCESS.2017.2683531.

[23] J. Zeng, B. Liu, and X. Su, "Joint pattern assignment and power allocation in PDMA," in *2017 IEEE 86th Vehicular Technology Conference (VTC-Fall)*, Sep. 2017, pp. 1–5, doi: 10.1109/VTCFall.2017.8288406.

[24] J. Zeng, X. Fan, Y. Zhong, M. Peng, T. Lv, and T. Jiang, "Downlink power allocation optimization in pattern division multiple access," *IEEE Access*, vol. 9, pp. 14649–14659, 2021, doi: 10.1109/ACCESS.2021.3049493.

[25] D. N. C. Tse and S. V. Hanly, "Multiaccess fading channels. I. Polymatroid structure, optimal resource allocation and throughput capacities," *IEEE Transactions on Information Theory*, vol. 44, no. 7, pp. 2796–2815, 1998, doi: 10.1109/18.737513.

[26] M. S. Ali, H. Tabassum, and E. Hossain, "Dynamic user clustering and power allocation for uplink and downlink non-orthogonal multiple access (NOMA) systems," *IEEE Access*, vol. 4, pp. 6325–6343, 2016, doi: 10.1109/ACCESS.2016.2604821.

BIOGRAPHIES OF AUTHORS

Linda Meylani received B.Eng. and M.Eng. in Telecommunication Engineering from Sekolah Tinggi Teknologi Telkom, Indonesia in 2002 and 2006 respectively. She received Ph.D. degree from Sekolah Teknik Elektro dan Informatika – Institut Teknologi Bandung (ITB) in 2021. From 2010, she joined The School of Electrical Engineering, Telkom University in The Telecommunication Engineering Program as a lecturer. Her research interest include wireless communication, multiple access, and information theory and coding. She can be contacted at lindameylani@telkomuniversity.ac.id.

Vinsensius Sigit Widhi Prabowo was born in Jakarta (Indonesia), 1993. He received the B.S. degree in Telecommunication engineering from Telkom University, Bandung, Indonesia, in 2015, M.S. degree in Electrical engineering from Telkom University, Bandung, Indonesia, in 2017. Since 2016, he is Tenured Lecturer with the School of Electrical Engineering, Telkom University. He is the author of "Pengalokasian Sumber Daya Radio pada Sistem Komunikasi Pita Lebar", and more than 20 indexed articles. His research interests include wireless communication system, radio resources management, and telecommunication transmission. He can be contacted at vinsensiusvsw@telkomuniversity.c.id.

Iswahyudi Hidayat received B.Eng. in Telecommunication Engineering from Sekolah Tinggi Teknologi Telkom, Bandung Indonesia in 2001 and received M.Eng. and Ph.D. from Institut Teknologi Bandung (ITB), Indonesia in 2007 anda 2022 respectively. Since 2002, he has joined as a lecturer at the Department of Electrical Engineering at Telkom University, formerly STT Telkom Bandung. His research area is in 5G and beyond (B5G) wireless communication systems, especially in non-orthogonal multiple access. He can be contacted at iswahyudihidayat@telkomuniversity.ac.id.

Nisa Alwiyah was born in Bandung (Indonesia), in 2001. She received Bachelor's Degree in Telecommunication Engineering at the School of Eletrical Engineering, Telkom University in 2023. She was a Research Assistant in the Communication System Laboratory. Her research interests include wireless communication, as well as the development of NOMA and 5G network schemes. She can be contacted at nisaalwiyah@gmail.com.